

PRE-1970 RC CORNER BEAM-COLUMN-SLAB JOINTS: SEISMIC ADEQUACY AND UPGRADABILITY WITH CFRP COMPOSITES

Murat Engindeniz¹, Lawrence F. Kahn², and Abdul-Hamid Zureick²

¹ Post-Doctoral Fellow, ² Professor

School of Civil and Environmental Engineering, Georgia Institute of Technology, Atlanta, GA, USA

Email: murat.engindeniz@gatech.edu

ABSTRACT:

This paper investigates experimentally the adequacy of corner beam-column joints in pre-1970 reinforced concrete buildings and determines the efficacy of carbon fiber-reinforced polymer (CFRP) composites for both pre- and post-earthquake retrofit of such joints. Four full-scale corner beam-column-slab specimens built with pre-1970 reinforcement details were subjected to a reverse-cycle bidirectional displacement history consisting of alternate and simultaneous cycles in the two primary frame directions before and/or after retrofit. Two of the specimens were first subjected to severe and moderate levels of damage, respectively, then repaired by epoxy injection, and strengthened by adding a #7 reinforcing bar within the clear cover at the column inside corner and by externally bonding multiple layers of CFRP to the beams, columns, and joint. Two other specimens were strengthened in their as-built condition. The results indicated that pre-1970 corner joints are severely inadequate to survive drift ratios of around 2% typically envisioned to occur during design earthquakes, and they cannot meet the FEMA 356 Life Safety and Collapse Prevention performance levels. It was shown, however, that such joints can be upgraded regardless of the level of existing earthquake damage to achieve a “rigid” joint behavior up to drift ratios of at least 2.4% applied simultaneously in both primary directions (i.e., 3.4% bidirectional drift) and to achieve joint shear strength factors larger than that used with seismically designed, code-conforming corner joints.

KEYWORDS: beam-column joint; reinforced concrete; fiber-reinforced polymer; retrofit; strengthening.

1. INTRODUCTION

In the United States, major developments pertaining to the evolution of seismic design provisions took place throughout the 1970s leading to improved codes and recommendations. Buildings constructed before the adoption of such documents, commonly referred to as the gravity-load-designed or pre-1970 buildings, constitute a significant portion of the building inventory in many countries and pose a significant risk for high economic and life losses in earthquakes. A major group of deficiencies in such buildings are in beam-column joint regions (Beres et al. 1996); these deficiencies lead to shear failure of exterior joints in earthquakes (Fig. 1a). The vulnerability is increased even more in the case of corner joints (Fig. 1b) since they are the least confined of all exterior joints and subjected to bidirectional shear demands. ACI 352R-02 (ACI-ASCE 2002) recommended further research to establish the adequacy of older joints, develop repair and strengthening techniques, and to study joints that are likely to be subjected to bidirectional loading.

Fiber-reinforced polymer (FRP) composites have exhibited great potential for seismic strengthening of beam-column joints in studies conducted since the late 1990's where significant data were obtained for FRP-retrofitted planar joint specimens (i.e., joints with no transverse beams or floor slab) subjected to unidirectional loads; those studies were reviewed elsewhere (Engindeniz et al. 2005). Promising results from such two-dimensional tests have recently led to more realistic testing of FRP-retrofitted beam-column joints as part of complete, full-scale framed structures (Di Ludovico et al. 2008). While recent studies have begun addressing the effects of actual 3D frame geometry and bidirectional loading on FRP-strengthening of beam-column joints, the effects of damage prior to retrofit have yet to be addressed. The need for further testing of FRP-retrofitted joints with realistic 3D geometry and loading conditions also stems from the fact that although the implementation of joint retrofit technology with FRPs has begun (Fig. 1c,d), the lack of comprehensive design guidelines prevents wider acceptance and implementation. Efforts to develop such guidelines for joints are currently underway in the ACI Committee 440.



Figure 1 – (a, b) Beam-column joint damages in 1999 İzmit, Turkey earthquake (Said and Nehdi 2004; Güney Özcebe 1999), and (c, d) implementation of FRP joint retrofit schemes in construction (Jorge Rendón 2007).

2. OUTLINE OF RESEARCH

This research focused on testing of corner beam-column joints before and after retrofit with CFRP composites. In particular, the research focused on five primary objectives:

1. Establish seismic adequacy of pre-1970 corner joints under bidirectional loading,
2. Investigate the efficacy of CFRP composites for: (a) post-earthquake retrofit such joints in cases of severe, moderate, or no existing damage, and (b) pre-earthquake retrofit in cases of moderate- or low-strength concrete, and
3. Ensure the applicability of the retrofit schemes to actual structures by accounting for the presence of floor members, and ensure the ease of retrofit construction by avoiding massive interventions to building appearance and occupancy such as those shown in Fig. 1d.

All tests were conducted on full-scale specimens representing the corner of a building isolated between two stories at the inflection points of beams and columns under lateral loading. A total of six tests were conducted on four specimens that were built to mimic pre-1970 design and construction practices according to the experimental program outlined in Table 1. The specimens were designed according to ACI 318-63 (ACI 1963) and by intentionally violating the current capacity design approach by targeting a column-to-beam strength ratio of 0.9. All specimens were identical in member sizes and steel reinforcement detailing which are shown in Fig. 2a. The specimens differed only in the concrete strength: Specimens 1, 2, and 3 had concrete strengths of 25.8, 34.6, and 33.9 MPa, respectively. Specimen 4 had a lower concrete strength of 15.4 MPa on the test day. The M10, M16, and M19 reinforcing bars had average yield strengths of 367, 352, and 315 MPa, respectively, and were characterized by the remarkable length of their yield plateaus (up to 1.8% strain for M19 bars).

Tests were conducted in a setup shown in Fig. 2b, where the base of the column had a fixed support, and the top of the column had a pin support with free vertical translation. Cyclic lateral loads were simulated by quasistatic cyclic loading of the beams in the vertical direction with the actuator-to-beam connections allowing free rotation around all three major axes (i.e., including torsion). Prior to cyclic loading, gravity load effects were accounted for by applying a column axial load of 10% of the column's compressive capacity, and then displacing both beams downwards until the strong-axis bending moments at the column faces were similar to those estimated for an actual building under service loads. The applied reverse-cycle displacement history consisted of alternate unidirectional loading up to $\pm 0.93\%$ interstory drift (θ) in each primary frame direction followed by simultaneous loading in both directions up to $\theta_{EW}=\theta_{NS}=\pm 3.7\%$ drift (i.e., bidirectional drift

Table 1 – Outline of experimental program.

Test	Specimen	Retrofit Scheme	Maximum Applied Interstory Drift, θ	
Test 1	Specimen 1	-	$\theta_{EW}=\theta_{NS}=\pm 1.9\%$	$\theta_b=[(\theta_{EW})^2+(\theta_{NS})^2]^{1/2}=\pm 2.7\%$
Test 2	Specimen 1	Scheme 1	$\theta_{EW}=\theta_{NS}=\pm 3.7\%$	$\theta_b=\pm 5.2\%$
Test 3	Specimen 2	-	$\theta_{EW}=\theta_{NS}=\pm 1.4\%$	$\theta_b=\pm 2.0\%$
Test 4	Specimen 2	Scheme 2	$\theta_{EW}=\theta_{NS}=\pm 3.7\%$	$\theta_b=\pm 5.2\%$
Test 5	Specimen 3	Scheme 2	$\theta_{EW}=\theta_{NS}=\pm 3.7\%$	$\theta_b=\pm 5.2\%$
Test 6	Specimen 4	Scheme 3	$\theta_{EW}=\theta_{NS}=\pm 3.7\%$	$\theta_b=\pm 5.2\%$

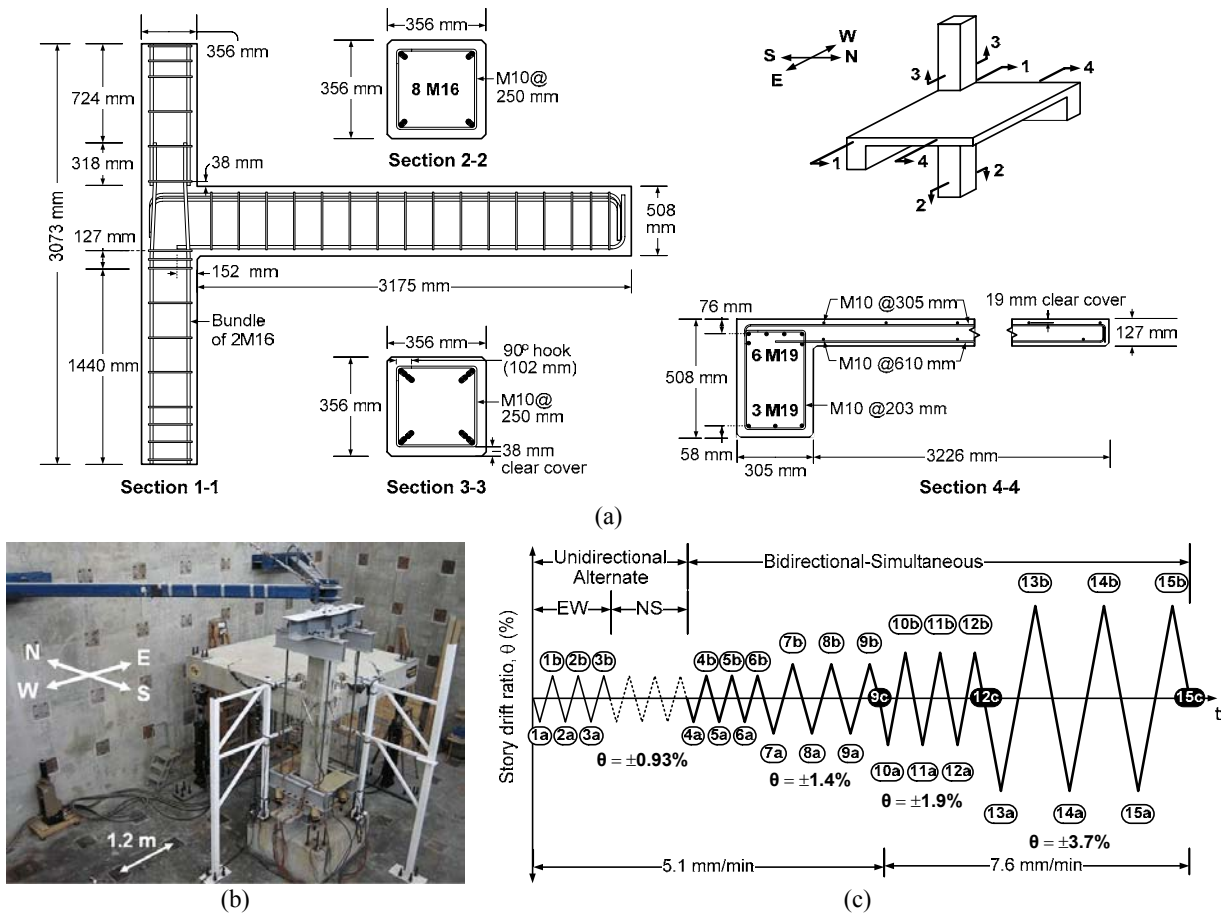


Figure 2 – (a) Reinforcement details, (b) test set-up, and (c) applied displacement history.

$\theta_b = \pm 5.2\%$) as shown in Fig. 2c. The applied displacement levels correspond to 1.0, 1.5, 2.0, and 4.0 times the displacement at first yield observed in Specimen 1 before retrofit. An extensive instrumentation layout consisting of 160 data acquisition channels was used. All details of the experimental program can be found elsewhere (Engindeniz 2008).

3. ADEQUACY OF AS-BUILT JOINTS

3.1. Damage Modes

The adequacy of the as-built joints was evaluated by testing Specimen 1 and Specimen 2 up to point 12c and point 9c in the loading history (Fig. 2c), respectively. During downward loading of the beams, damage modes included extensive yielding in the column bars especially at the inside (NE) corner with limited or no yielding in beam top bars, joint shear cracking and large joint shear rotations, and bulging of the joint panels. When the beams were loaded upwards, the loss of anchorage of beam bottom bars was solely responsible for the poor behavior. Such bond failure was why the cracking in the joint panels was along one diagonal only, and not in the often observed “X” pattern. These unfavorable damage modes were so dominant that, at the $\pm 1.9\%$ drift level ($\theta_b = \pm 2.7\%$) applied to Specimen 1, up to 70% of the beam end displacement during downward was caused by joint shear rotations, and 100% of that during upward loading was caused by the loss of anchorage of beam bottom bars as quantified by Engindeniz (2008). Much of the damage progression in Specimen 1 took place during the $\pm 1.9\%$ drift cycles ($\theta_b = \pm 2.7\%$) where the diagonal joint shear cracks tripled in width and extended vertically into the upper column causing the loss of anchorage of lap-spliced column bars (Fig. 3a). Even at a lower drift level of $\pm 1.4\%$ ($\theta_b = \pm 2.0\%$), however, joint shear cracking and the anchorage loss of beam bottom bars were significant as seen from the state of damage in Specimen 2 at the end of its testing (Fig. 3b).

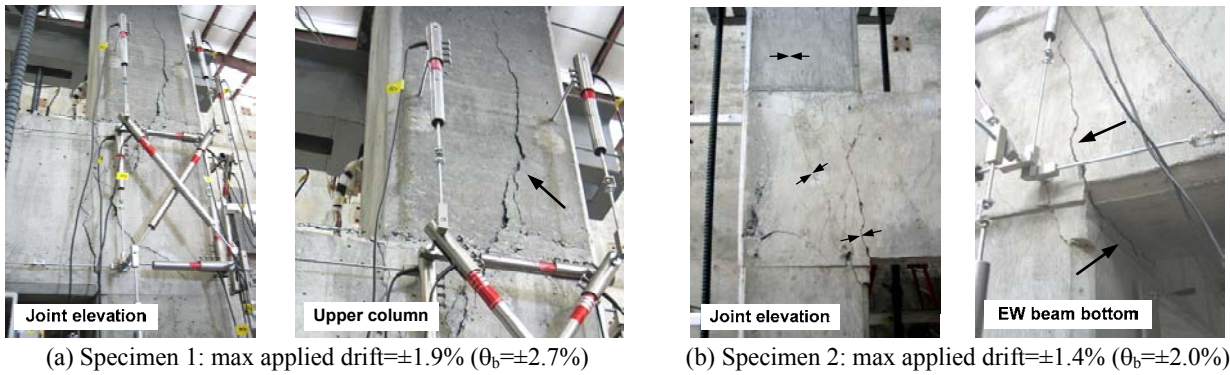


Figure 3 – Damage modes before retrofit.

3.2. Hysteretic Behavior

The aforementioned damage mechanisms resulted in force-drift hysteretic curves characterized by lack of ductility due to severe degradation in stiffness, pinching, and loss of strength especially after the beginning of the bidirectional cycles. The curves obtained for the NS beam in Specimen 1, for example, are shown with solid lines in Fig. 4a. The curves are shifted from the horizontal line representing zero load due to the initial compressive (positive) loads on the actuators at the simulated service load level.

The peak-to-peak stiffness K_p , defined as the slope of the line connecting the negative and positive peaks of a cycle, decreased by 78% from the first to the last (12th) cycle for Specimen 1. For Specimen 2, the decrease in K_p until the last (9th) cycle was 52%. No effective energy dissipation mechanisms were developed in either specimen because of the progressive increase in pinching and strength degradation.

3.3. Joint Shear Strength

Specimens 1 and 2 were found to carry a maximum normalized joint shear stress τ' of $0.67\sqrt{\text{MPa}}$ in a primary frame direction (τ'_{EW} or τ'_{NS}) and 0.90 and $0.91\sqrt{\text{MPa}}$ in an approximately 45-degree direction from the beam axes (i.e., $\tau'_b = [(\tau'_{EW})^2 + (\tau'_{NS})^2]^{1/2}$). These values were obtained not by considering the contribution of strong-axis beam moments only as typically done for planar joints, but by considering all forces transferred to the joint by the beam top bars as quantified from the strains measured in them. The fact that the maximum τ'_b values were close to the shear strength factor of $\gamma=1.0$ recommended by ACI 352R-02 for well-detailed corner joints is because of the conservatism of the ACI 352R-02 in assuming a circular interaction diagram for the case of bidirectional loading, and not because the tested specimens exhibited behaviors comparable to those of well-detailed joints.

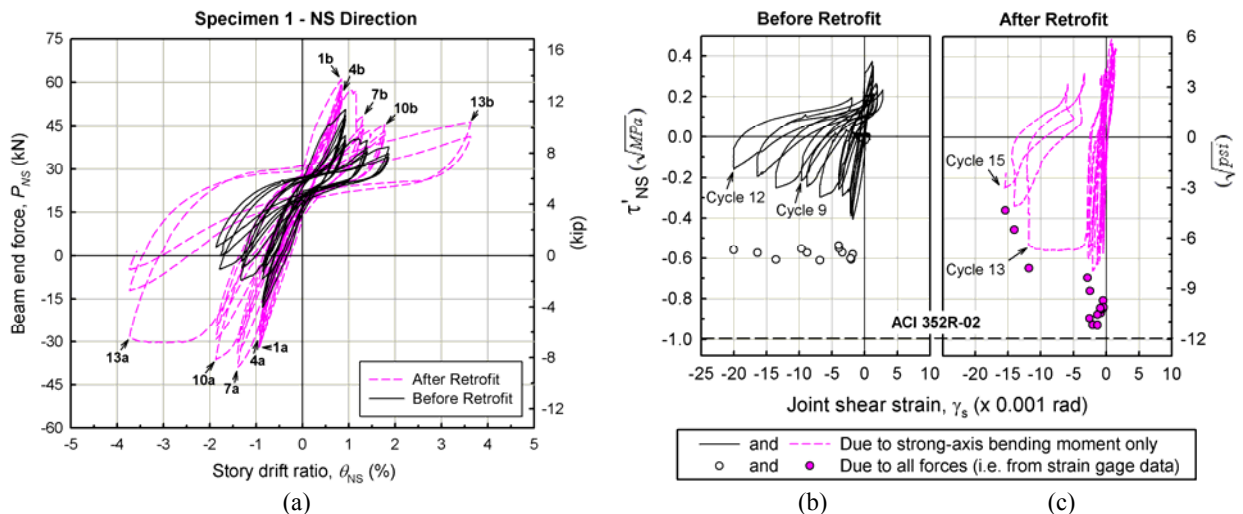


Figure 4 – Hysteretic behavior of Specimen 1, NS direction: (a) force-drift, and (b, c) joint shear stress-strain.

The increase in the joint shear stresses caused by the bidirectional nature of loading and the presence of slab was also quantified. When τ'_b values were obtained by considering the contribution of strong-axis bending moments only, it was found that 53% and 41% of the aforementioned maximum τ'_b values for Specimen 1 and Specimen 2 were caused by tension in slab reinforcement and the resulting torsion. Increases in joint shear stresses due to such three-dimensional effects were confirmed analytically by Engindeniz (2008).

While the method of considering the strong-axis bending moments only does not accurately estimate the joint shear strength, it provides an effective means to plot the hysteretic variation of normalized joint shear stress τ' versus joint shear strain γ_s as shown with solid black curves in Fig. 4b for Specimen 1 NS direction. From these curves, it was clear that the joint was far from being “rigid” during downward loading as evidenced by joint shear strains up to -0.02 rad, and unable to mobilize any resistance during upward loading due to pull-out of beam bottom bars. These findings, coupled by the aforementioned damage modes and the resulting deficiencies in stiffness and energy dissipation indicated the need for significant shear strengthening of the joint to achieve an ideal “rigid” joint behavior.

4. RETROFIT APPROACH

The retrofit procedure consisted of three steps. In Step 1, which was applied only to the previously damaged Specimens 1 and 2, all cracks wider than 0.3 mm were injected with a high-modulus, low-viscosity epoxy. In Step 2, the column inside (NE) corner was strengthened for flexure to delay/prevent the observed extensive localized yielding at this corner. A 50 mm x 50 mm portion of the column inside corner was removed, including a small perforation in the slab, a M22 (#7) steel reinforcing bar with $f_y=445$ MPa was added, and a polymer-modified cementitious mortar ($f_c=49.6$ MPa) was cast (Fig. 5a). In Step 3, a multi-layer CFRP system tailored from a relatively light (300 g/m²) unidirectional carbon fabric was bonded externally to improve the joint shear strength, positive moment capacity of the beam (i.e., beam bottom bar anchorage), and confinement of the column and beam ends. The CFRP had the following design properties: tensile strength=370 N/mm/layer, ultimate strain=1.00%, and thickness=0.5 mm/layer.

While Step 2 was identical for all specimens, modifications were made to the CFRP schemes used in Step 3 to maximize the improvements in behavior as the testing program progressed. This resulted in the use of three different CFRP schemes as listed in Table 1 and one of which (Scheme 2) is shown in Fig. 5b. In this particular scheme, three 90° (perpendicular to column axis) and two 0° layers were used in the joint panels and extended onto the columns to increase the joint shear strength, five layers of 180 mm-wide CFRP strips were placed around the outside corner of the joint and extended onto both beams 2080 mm to delay/prevent the loss of anchorage of beam bottom bars, the beam ends were U-wrapped with two layers to prevent debonding of these strips, and the column ends were fully wrapped with two layers to improve ductility, improve the anchorage of the sheets extended from the joint panels, and to improve the anchorage of the steel reinforcing bar added at the inside corner of the column. The CFRP layups labeled 1 through 7 in Fig. 5b represent the combination of all these CFRP sheets stacked in a sequence that would result in a symmetric layup in all areas. The differences between the three schemes are also listed in Fig. 5b. In Scheme 1, used for Specimen 1, the horizontal strips placed around the joint were extended onto the beams by only 710 mm with no beam U-wrapping.

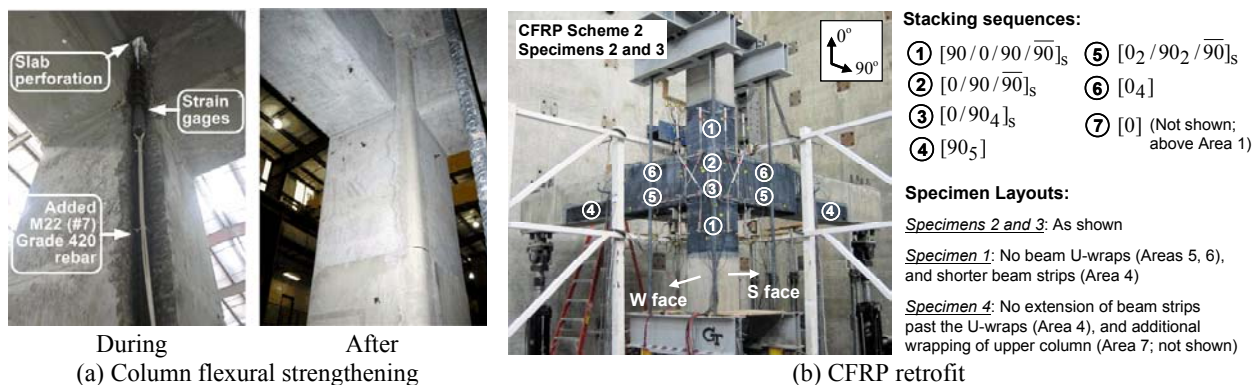


Figure 5 – Retrofit procedure.

In Scheme 3 (Specimen 4), the extension of the horizontal strips past the U-wrapped portion was eliminated, and the upper portion of the upper column was also wrapped with one layer to improve the low column shear strength in that specimen. All CFRP-applied areas were heat-cured at $80\pm 10^{\circ}\text{C}$ for 6 hours following the application to quickly achieve the full-cure of the epoxy resin and to increase its glass-transition temperature; this curing schedule was selected based on the differential scanning calorimetry tests conducted on the resin prior to the application. Engindeniz (2008) gives all details of the retrofit designs.

5. EFFECT OF EXISTING DAMAGE LEVEL ON THE EFFICACY OF RETROFIT

The effect of the level of existing damage on the efficacy of CFRP retrofit was investigated based on the data obtained from retesting of Specimens 1 and 2 after retrofit, and from testing of Specimen 3 which was retrofitted in its undamaged state.

The severely damaged Specimen 1 was retrofitted with the first (preliminary) CFRP scheme tested, and that retrofit scheme's performance does not necessarily represent the best upgradability of a severely damaged joint with CFRPs. Yet, the results were promising. During downward loading, a ductile beam hinge was formed (Fig. 6a), which was manifested in the lower half of force-drift hysteretic curves with significantly higher peak loads and increased energy dissipation capacity (Fig. 4a). The joint exhibited a "rigid" behavior up to a drift of $\theta_{EW}=\theta_{NS}=-2.4\%$ ($\theta_b=-3.4\%$) and was able to withstand a maximum normalized joint shear stress of $\tau'_b=1.29\sqrt{\text{MPa}}$ which is larger than $\gamma_{ACI352}=1.0$. Improvements in the case of upward loading, however, were not sufficient. The CFRP beam strips used for preventing the pull-out of beam bottom bars debonded early at peaks 7b and 10b ($\theta_{EW}=\theta_{NS}=1.4-1.9\%$; $\theta_b=2.0-2.7\%$) in the NS and EW directions (Fig. 6a), respectively. Debonding resulted in a significant reduction in strength, stiffness, and energy dissipation as seen in the upper half of the hysteretic curves in Fig. 4a. In summary, the results of Specimen 1 indicated that even a severely damaged corner joint could be retrofitted effectively if the anchorage of the CFRP beam strips in Scheme 1 was improved.

Modifications created the improved Scheme 2 (Fig. 5b): longer extension lengths of beam strips (areas 4 and 5), and U-wrapping of these strips near the beam ends (areas 5 and 6). The efficacy of Scheme 2 was then tested on the previously moderately damaged Specimen 2, and on the undamaged Specimen 3. These two tests allowed direct assessment of the effect of prior damage on the efficacy of the CFRP retrofit since Specimens 2 and 3 were identical, even in terms of concrete strength (same batch). Scheme 2 eliminated the drawbacks of Scheme 1 up to a drift ratio of $\theta_{EW}=\theta_{NS}=+2.6\%$ ($\theta_b=+3.7\%$) toward peak 13b at which point the full capacity (rupture) of the CFRP beam strips placed around joint was developed (Fig. 6b,c), and the seismically desired beam positive moment capacity of at least half the negative moment capacity was achieved. The previously damaged Specimen 2 exhibited an additional 22% increase in the peak loads in the upper half of the force-drift hysteretic curves and a 21% increase in the overall energy dissipation compared to the values obtained for the retrofitted Specimen 1 (Fig. 7a vs. Fig. 4a). The ductility of the beam negative moment hinges that formed during downward loading was also remarkable with the beam top bars mobilizing their entire yield plateaus.

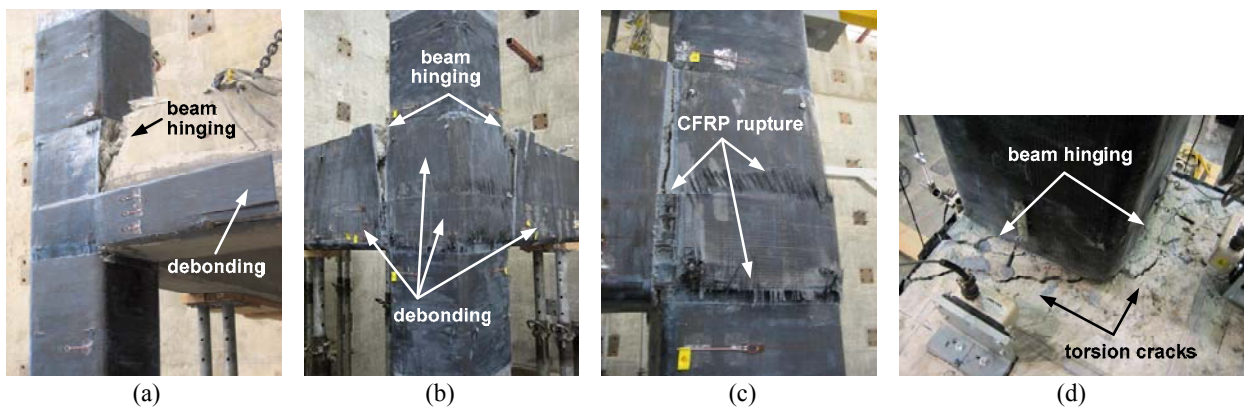


Figure 6 – Damage modes after retrofit: (a) Specimen 1, (b, c) Specimen 2, and (d) Specimen 3.

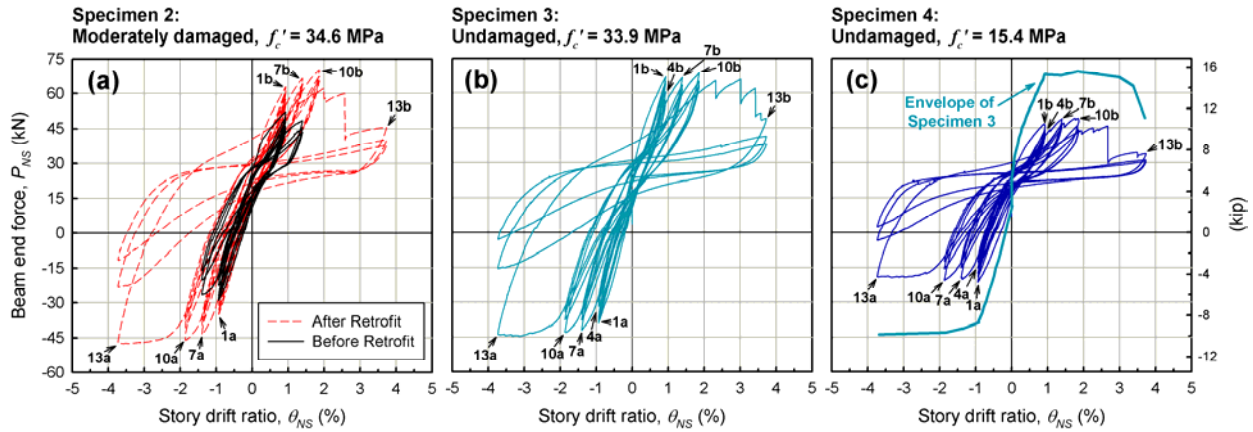


Figure 7 – Force-drift hysteretic response of Specimens 2, 3, and 4 in the NS direction.

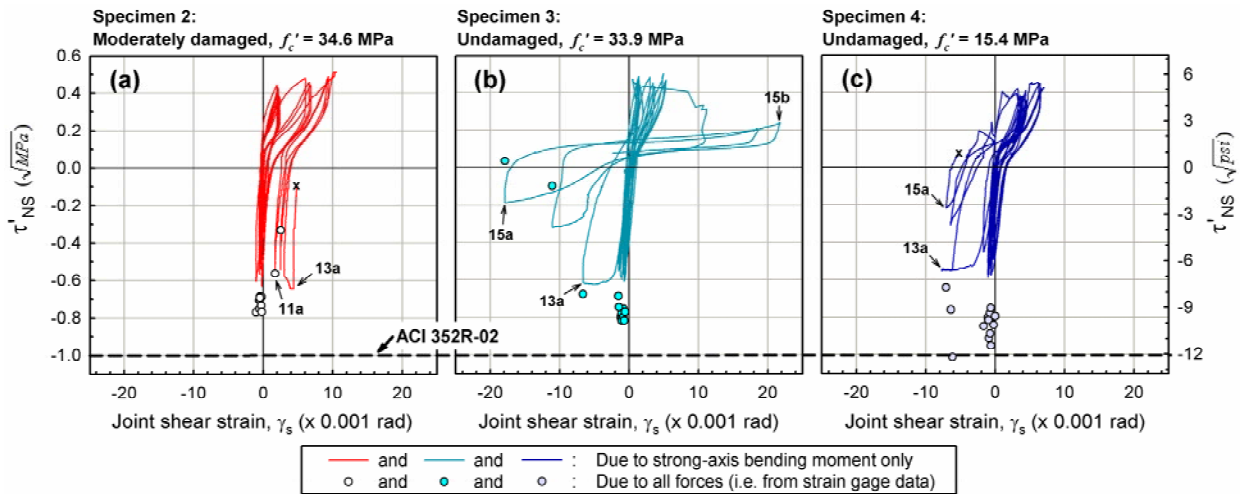


Figure 8 – Normalized joint shear stress-strain hysteresis loops of Specimens 2, 3, and 4 in the NS direction.

When Scheme 2 was applied to the undamaged Specimen 3, the additional improvements in the force-drift response compared to that of Specimen 2 were limited to an 8% increase in the initial stiffness, up to 10% increase in peak loads in the first three cycles, a more progressive failure of CFRP toward peak 13b, and a resulting increase in the energy dissipation capacity of only 2% (Fig. 7b vs. Fig. 7a). The increase in the joint shear strength was also limited; an 8% additional increase was obtained over that of Specimen 2 ($\tau'_b = 1.15\sqrt{\text{MPa}}$ vs. $1.06\sqrt{\text{MPa}}$). Such changes did not indicate a clear benefit of pre- over post-damage retrofit. Pre-damage retrofit showed improved behavior in that the joint was able to maintain much of its improved strength through larger drift levels as evident from a comparison of Fig. 8a and Fig. 8b. While the previously damaged Specimen 2 lost it much of its improved strength after cycle 10 ($\theta_{EW} = \theta_{NS} = 1.9\%$; $\theta_b = 2.7\%$), the undamaged Specimen 3 exhibited a τ'_b value of $1.03\sqrt{\text{MPa}}$ even at peak 13a ($\theta_{EW} = \theta_{NS} = -3.7\%$; $\theta_b = -5.2\%$).

6. PRE-EARTHQUAKE RETROFIT IN THE CASE OF LOW-STRENGTH CONCRETE

The effect of low-strength concrete on the efficacy of pre-earthquake retrofit was studied by comparing the response of Specimen 4 ($f'_c = 15.4 \text{ MPa}$) to that of Specimen 3 ($f'_c = 33.9 \text{ MPa}$). To allow such a comparison, the modifications made to Scheme 2 to arrive at Scheme 3 were kept to a minimum as described in Sec. 4, although low f'_c implied a reduction in column-to-beam strength ratio, reduction in all shear capacities including that of the joint, and worsening of anchorages of both the reinforcing bars and CFRP sheets.

Despite the low f'_c , Specimen 4 withstood a maximum normalized joint shear stress of $\tau'_b=1.41\sqrt{\text{MPa}}$ which was the largest value obtained in this project (Fig. 8c) and which was 41% larger than $\gamma_{\text{ACI352}}=1.0$. The CFRP-to-concrete bond was not any worse; complete debonding of the joint sheets did not occur any earlier; and rupture of the beam strips was still achieved. Such a remarkable joint response, however, did not translate into an acceptable overall behavior. All force-drift response parameters were significantly reduced relative to those of Specimen 3 as shown in Fig. 7c. The peak-to-peak stiffness of Specimen 4 was not only 32 to 44% lower than that of Specimen 3 throughout the test, it was also 15 to 20% lower than that of the as-built Specimen 2. The cumulative dissipated energy was 37% less than that of Specimen 3. Such reduced overall properties were due to the fact that a strong column/weak beam behavior could not be achieved because of the lower column-to-beam strength ratio and reduced anchorage of beam top bars within the joint. It was concluded that in such cases of low f'_c , more invasive techniques may be necessary to improve the overall lateral stiffness and the reinforcement anchorages so that the improved joint strength can be mobilized.

7. CONCLUSIONS

Four full-scale RC beam-column-slab joint specimens representing typical pre-1970 design were subjected to cyclic bidirectional loading before and/or after retrofit with CFRP composites. The following conclusions were drawn from the results of these experiments:

1. Pre-1970 corner beam-column joints were found to be severely inadequate in meeting seismic demands because of column bar yielding, joint shear failure, loss of anchorage of beam bottom bars, failure of column lap-splices, and the resulting loss of stiffness and strength that dominated their behavior even at interstory drift levels lower than those envisioned to occur during typical design earthquakes (i.e., ~2%). Bidirectional loading increased joint shear stresses and exacerbated deterioration.
2. Regardless of the level of existing damage and concrete strength, CFRP composites provided an effective and easy-to-implement means to improve the shear strength of all tested joints to above $1.0\sqrt{\text{MPa}}$ which is required for code-conforming corner joints. A “rigid” joint behavior was achieved even for a severely-damaged-then-retrofitted specimen up to a drift ratio of $\theta_{\text{EW}}=\theta_{\text{NS}}=2.4\%$ ($\theta_b=3.4\%$).
3. Post-earthquake retrofit was as effective as pre-earthquake retrofit in achieving a strong column/weak beam behavior and in improving the joint behavior; however, much of the improved joint shear strength could be maintained through larger drift levels (up to $\theta_{\text{EW}}=\theta_{\text{NS}}=3.7\%$; $\theta_b=5.2\%$) only in the case of pre-earthquake retrofit.
4. Low-strength concrete (15 MPa) did not hinder the efficacy of CFRPs for improving the joint shear strength in the case of pre-earthquake retrofit but did cause a significant reduction in the overall stiffness of the specimen which prevented the formation of a beam hinging mechanism.

REFERENCES

- ACI Committee 318 (1963). Building Code Requirements for Reinforced Concrete (ACI 318-63), American Concrete Institute, Detroit, MI.
- ACI-ASCE Committee 352 (2002). Recommendations for Design of Beam-Column Connections in Monolithic Reinforced Concrete Structures (ACI 352R-02), American Concrete Institute, Farmington Hills, MI.
- Beres, A., Pessiki, S. P., White, R. N., and Gergely, P. (1996). Implications of experiments on the seismic behavior of gravity load designed RC beam-to-column connections. *Earthquake Spectra* **12:2**, 185-198.
- Di Ludovico, M., Prota, A., Manfredi, G., and Cosenza, E. (2008). Seismic strengthening of an under-designed RC structure with FRP. *Journal of Earthquake Engineering and Structural Dynamics* **37:1**, 141-162.
- Engindeniz, M., Kahn, L. F., and Zureick, A. (2005). Repair and strengthening of reinforced concrete beam-column joints: State of the art. *ACI Structural Journal* **102:2**, 187-197.
- Engindeniz, M. (2008). Repair and Strengthening of Pre-1970 Reinforced Concrete Corner Beam-Column Joints Using CFRP Composites. Ph.D. thesis, Georgia Institute of Technology, Atlanta, GA. Available online at <http://etd.gatech.edu>.
- Said, A. M., and Nehdi, M. L. (2004). Use of FRP for RC frames in seismic zones: Part I. Evaluation of FRP beam-column joint rehabilitation techniques. *Applied Composite Materials* **11:4**, 205-226.